Effects of acupuncture at HT7 on glucose metabolism in a rat model of Alzheimer's disease: an ^{18}F-FDG-PET study

Xinsheng Lai,[1] Jie Ren,[2] Yangjia Lu,[2,3] Shaoyang Cui,[1,4] Junqi Chen,[2,5] Yong Huang,[2] Chunzhi Tang,[1] Baoci Shan,[6] Bingbing Nie[6]

[1]Department of Acupuncture and Massage, Guangzhou University of Traditional Chinese Medicine, Guangzhou, China
[2]School of Traditional Chinese Medicine, Southern Medical University, Guangzhou, China
[3]Department of Traditional Chinese Medicine, Guangdong Medical College, Dongguan, China
[4]Department of Acupuncture and Moxibustion, Futian TCM Hospital, Shenzhen, China
[5]Department of Rehabilitation, The 3rd affiliated Hospital of Southern Medical University, Guangzhou, China
[6]Key Laboratory of Nuclear Analytical Techniques, Institute of High Energy Physics, Chinese Academy of Sciences, Beijing, China

Correspondence to
Dr Yong Huang, School of Traditional Chinese Medicine, Southern Medical University, No. 1023, Shatai Road, Guangzhou 510515, China;
nanfanglihuang@163.com

XL and JR are joint first authors and contributed equally.

Accepted 8 November 2015
Published Online First
9 December 2015

To cite: Lai X, Ren J, Lu Y, *et al*. *Acupunct Med* 2016;**34**:215–222.

ABSTRACT

Objective To explore the effects of acupuncture at HT7 on different cerebral regions in a rat model of Alzheimer's disease (AD) with the application of ^{18}F-2-fluoro-deoxy-D-glucose positron emission tomography (FDG-PET).

Methods Sixty Wistar rats were included after undergoing a Y-maze electric sensitivity test. Ten rats were used as a healthy control group. The remaining 50 rats were injected stereotaxically with ibotenic acid into the right nucleus basalis magnocellularis and injected intraperitoneally with D-galactose. AD was successfully modelled in 36 rats, which were randomly divided into three groups (n=12 each): the AD group, which remained untreated; the AD+HT7 group, which received 20 sessions of acupuncture at HT7 over 1 month; and the AD+Sham group, which received acupuncture at a distant non-acupuncture point. Total reaction time (TRT) was measured by Y-maze and ^{18}F-FDG-PET scans were conducted on day 1 and 30. PET images were processed with Statistical Parametric Mapping 8.0.

Results Pre-treatment, TRT was greater in all AD groups versus controls (mean±SD 24.10 ±2.48 vs 41.34±5.00 s). Post-treatment, TRT was shortened in AD+HT7 versus AD+Sham and AD groups ($p<0.0001$, two-way analysis of variance). Glucose metabolic activity in the hippocampus, thalamus, hypothalamus, frontal lobe, and temporal lobe was decreased in AD rats compared with healthy controls and relatively elevated after HT7 acupuncture. Compared with sham acupuncture, HT7 needling had a greater positive influence on brain glucose metabolism.

Conclusions Needling at HT7 can improve memory ability and cerebral glucose metabolic activity of the hippocampus, thalamus, hypothalamus, and frontal/temporal lobes in an AD rat model.

INTRODUCTION

Alzheimer's disease (AD), the most common cause of dementia, is a primary neurodegenerative brain disease characterised by global cognitive decline including impairment of memory and reasoning ability.[1 2] Pathological changes in the brain consist of abundant extracellular β-amyloid (Aβ) plaques, (congophilic) cerebral amyloid angiopathy (CAA), and neurofibrillary tangles (NFTs).[3 4] Despite an extensive research focus on AD, there is still no effective treatment to slow its progression.

Acupuncture, a classical treatment that has been practised as one component of Traditional Chinese Medicine (TCM) for more than 3000 years, has become one of the most popular forms of complementary medicine for neurodegenerative diseases and may be an effective treatment for AD.[5 6] Several studies have shown that patients treated with acupuncture demonstrated an improvement in verbal orientation and motor coordination and had higher overall scores on the mini-mental state examination (MMSE) and AD assessment scale-cognitive section (ADAS-Cog).[5 7] In animal models of AD, acupuncture has been shown to enhance cholinergic neurotransmission and release of trophic factors, reduce oxidative damage, improve synaptic plasticity, and decrease levels of Aβ proteins in the hippocampus and other relevant brain regions.[8] In spite of increasing acupuncture usage, the neural mechanisms underlying its therapeutic effects are still not well understood. Factors that may affect the efficacy

of acupuncture for the treatment of AD include stage of the disease, selection of the acupuncture points, and methods of needle insertion and/or stimulation. Historically, the point HT7 (*Shenmen*) has been used to treat irritability, psychosis, epilepsy, poor memory, palpitations, and insomnia. It may improve brain (especially prefrontal) functions, such as memory, attention, vocalisation, and project abilities, and has been widely applied for AD, in which therapeutic effects have been shown.[9]

Positron emission tomography (PET), a non-invasive functional imaging approach, provides a unique insight into the neuropathological changes in specific cerebral region in AD.[10 11] Recently, ^{18}F-2-fluoro-deoxy-D-glucose (FDG)-PET has been applied to measure cerebral rates of glucose metabolism (CMRglcs) which is considered to be an imaging biomarker with good sensitivity in the early diagnosis of AD.[12]

In this study, we explored the effects of AD on memory in a rat model with the application of a Y-maze test. Using ^{18}F-FDG-PET, we also aimed to identify brain regions demonstrating altered cerebral glucose metabolism activity to examine the mechanisms of action of needling at HT7.

METHODS

Experimental animals

Eighty 2-month-old Wistar rats weighing 200–250 g were provided by the animal centre of the China Academy of Chinese Medical Sciences. All experimental procedures were carried out in accordance with the Guidelines for the Care and Use of Laboratory Animals of the Ministry of Science and Technology of the People's Republic of China and were approved by the Committee on Ethical Use of Animals of Guangzhou University of Chinese Medicine (reference no. SPF20110032).

All rats underwent an initial screening test using a Y-maze task with a fixed training time, which was carried out by a professional technician under quiet and dim light conditions. Each rat was placed in an arm facing the centre and was allowed to freely explore the maze for 5 min. The 'safe zone' and 'electric shock zone' were regularly alternated. A total of 20 rats with hypersensitive or insensitive reaction to electric shocks were excluded from the study.

AD model establishment

The remaining 60 rats were housed 2–3 per cage in a room with a 12 h light/12 h dark cycle (lights on 07:00–19:00). Room temperature and humidity were set at 18–22°C and 40–70%, respectively.

After 1 week of acclimatisation, rats were randomly divided into a control group (n=10) and a model group (n=50). The latter group of rats received daily intraperitoneal injections of 4.2 mg/kg D-galactose (D-gal) dissolved in 0.9% saline (20 mg in 2 mL) for a total of 6 weeks. In the seventh week, rats in the model group were anaesthetised with intraperitoneal sodium pentobarbital (50 mg/kg), placed on a stereotaxic apparatus, and given an injection of 1 µL ibotenic acid (IBO) into the right nucleus basalis magnocellularis (NBM) 0.9 mm posterior and 2.8 mm lateral to the bregma and 6.9 mm vertically from the skull surface. Stereotaxic coordinates were set at AP (anteroposterior) 0.8 mm, Lat (lateral) 2.6 mm, DV (dorsoventral) 8.2 mm. IBO was dissolved in 0.9% saline at a concentration of 8 µg/µL and bilateral infusions of 1 µL IBO were administered into the NBM (using a 5 µL Hamilton syringe) over a period of 5 min. The needle was left in place for 10 min after completing the infusion. Control group rats were infused with 1 µL 0.9% saline using the same procedure. After the operation, all rats received benzylpenicillin sodium for 3 days.

Two weeks after injection, all rats underwent a spatial learning and memory test using the same Y-maze task as used for screening, wherein electric shocks were applied to enhanced the rats' ability to distinguish light stimulation and the location of the safe zone. Each electric shock lasted 5 s (voltage 50–70 V). A correct reaction occurred when the rat moved to the safe zone within 10s of an electric shock without retracing its steps. A specific method was used in which the safe zone (arm) was altered in the order A-B-C-A. Once the rat reached the safe zone, it was exposed to light stimulation for 15 s, which counted as one test. The arm in which the rat stayed was regarded as the starting arm of the next test, which began after a break of 30 s. This process was repeated 20 times a day. The total reaction time (TRT) of each rat was recorded each day. The average upper limit of TRT in the control group (95–99%) was defined as the standard for successful induction of the AD model, and was achieved in 36 of 50 rats.

Acupuncture treatment

The 36 successfully modelled rats were divided into three groups (n=12 each using random number tables): the AD group, which remained untreated; the AD+HT7 group, which received acupuncture at HT7; and the AD+Sham group, which received (penetrating) acupuncture at a non-acupuncture point.

All acupuncture treatments were provided by a single skilled acupuncturist. Rats in the AD+HT7 group were needled at the HT7 acupuncture point on the left forelimb, which was located on the wrist crease, at the edge of the ulna.[13] In the AD+Sham group, rats received acupuncture at a point located 5 mm below the left capitulum fibula, 2 mm to the right. Sterile disposable stainless steel needles (length 9 mm, diameter 0.18 mm; Hwato, Suzhou Medical Supplies Factory Co, Ltd., China) were used in this study. Rats in the control and (untreated) AD groups did not receive any acupuncture intervention but were handled and fixed in the same way as the two groups

that received treatment. Acupuncture needles were inserted perpendicularly to a depth of 3 mm and twisted/rotated at a frequency of 120–150 times per min for 3 min. This was followed by a 2 min break and the process was repeated three times. Acupuncture treatments were repeated on 5 days per week until completion of the study on day 30.

^{18}FDG-PET imaging

Cerebral images were acquired using PET during the first and final acupuncture sessions on day 1 and day 30. After 24 h of fasting, blood glucose values were measured from tail bleeds by the glucose oxidase method (Glucose Kit, bioMerieux, normal standard 3.95±1.31 mmol/L) before the rats were sent for PET scanning at the PET-CT Centre of the Experimental Animals Center of the People's Liberation Army (PLA) General Hospital. A tracer (fludeoxyglucose (18F)), ^{18}F-FDG, synthesised with Mini Tracer accelerator, 1.5 mci/500 g dosage) was injected via the tail vein 3 min after the start of the first acupuncture treatment, which continued for the next 10 min post-injection. After the treatment, rats were anaesthetised with 5% isoflurane in 100% oxygen 5 min before the scan.

FDG-PET images were acquired using a Siemens Inveon PET system (Siemens Medical Solutions) with a radial spatial resolution of 1.4 mm full-width at half-maximum (FWHM) at the centre of the field of view (FOV). Images were subsequently reconstructed using a filtered back projection (FBP) algorithm on a 128×128×159 matrix, where the voxel size equals 1.46×1.46×0.79. All scans were saved in Analyse 7.5 format.

Imaging was repeated on day 30, after completion of the 20th acupuncture treatment. After scanning, the Y-maze test of spatial learning and memory was also repeated and the final TRT of each group was recorded.

Statistical analysis and image processing

Y-maze data were expressed as mean±SD, and were processed with the Statistical Package for the Social Sciences V.13.0 (SPSS Inc, Chicago, Illinois, USA) using two-way analysis of variance (ANOVA) followed by Tukey's post hoc test. Formal statistical significance was reached when $p<0.05$.

The PET images of the rat brain were analysed using a Statistical Parametric Mapping 8.0 (SPM8) toolbox called SPMratIHEP.[14] Images were preprocessed using spatial normalisation and smoothing. All the FDG-PET functional images were normalised to the PET template of the rat brain in SPMratIHEP to eliminate individual differences, and then resliced by 1.0×1.0×2.0 mm^3 voxels. Within this step, the intracranial tissue of the individuals were extracted out automatically, and standardised into the Paxinos and Watson[15] rat brain axis. In addition, the spatially normalised functional images were smoothed by a Gaussian kernel of 2×2×4 mm^3 FWHM. Then, the preprocessed images were statistically analysed voxel-by-voxel within SPMratIHEP based on the framework of the general linear model. In order to identify differences in FDG signals between the two groups, a two-sample t test was performed. Proportional scaling was applied to account for global confounders. Brain regions with significant FDG changes in the AD rats were yielded based on a voxel-level height threshold of $p<0.001$ (uncorrected) and a cluster-extent threshold of 100 voxels.

RESULTS

Y-Maze test

As shown in figure 1, before treatment, TRT was significantly increased in the 36 successfully modelled rats compared to the control group (41.34±5.00 vs 24.10±2.48 s, $p<0.0001$) and was balanced between AD, AD+Sham and AD+HT7 groups, with no significant differences between the three groups at baseline ($p>0.05$). After completing 20 sessions of acupuncture treatment, TRT in the AD+HT7 group was significant lower than the AD and AD+Sham groups (30.40±2.99 vs 44.06±4.65 s and 42.05 ±2.81 s, respectively, $p<0.0001$). By contrast there were no significant differences in TRT after treatment in the AD+Sham versus AD groups. Moreover, measures of TRT remained higher in all three AD groups relative to the control group on day 30 ($p<0.0001$).

Changes in glucose metabolism in different brain regions

Tables 1–3 detail the specific brain regions in which a significant elevation in cerebral glucose metabolism was observed in control versus AD, AD+HT7 versus AD, and AD+HT7 versus AD+Sham groups, respectively. Significance is reflected by the maximum t value (Max_T) in each cluster, and location is given by the

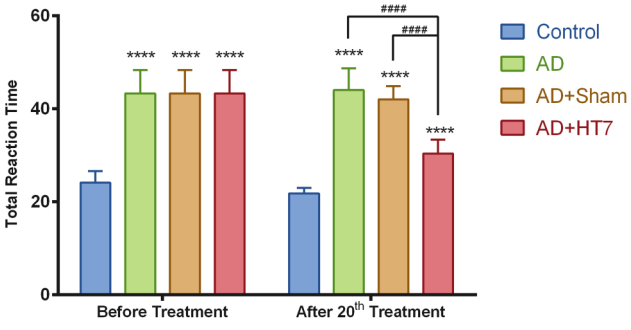

Figure 1 Total reaction time, measured as part of a Y-maze task, in 10 healthy rats (control group, n=10) and 36 rats with Alzheimer's disease (AD) left untreated (AD group, n=12) or treated with 20 sessions of acupuncture at HT7 (AD+HT7 group, n=12) or a distant non-acupuncture point (AD+Sham group, n=12) over a 30-day period. Data are mean±SD. ****p<0.0001 compared to control group; ####p<0.0001 compared to AD+HT7 group.

Table 1 Brain regions demonstrating increased cerebral glucose metabolism in control versus Alzheimer's disease (AD) groups

Anatomical structure	Max_T	Peak coordinates (mm) X	Y	Z
Day 1				
Bed nucleus of stria terminalis	3.93	−1.48	6.00	−0.36
Cingulate gyrus	3.75	−0.27	2.72	−0.36
Dorsal thalamus—lateral nucleus group	3.94	−1.45	6.91	−2.28
Hippocampus	5.03	4.86	3.37	−4.44
Insular cortex	3.98	−3.80	4.95	3.48
Orbital cortex	4.85	−3.40	5.26	3.48
Piriform cortex	4.78	−3.13	6.01	3.48
Sensory cortex	3.75	−3.48	2.09	−0.36
Striatum	4.41	−2.29	2.70	0.12
Day 30				
Auditory cortex	4.18	6.45	5.30	−3.72
Cingulate gyrus	4.85	0.09	3.11	2.04
Dorsal thalamus—lateral nucleus group	4.24	−1.59	6.44	−2.04
Hippocampus	3.86	−5.96	5.56	−4.92
Midbrain—inferior colliculus	3.54	−2.85	4.95	−7.56
Midbrain—tegmentum of midbrain	3.63	−2.84	5.56	−7.80
Piriform cortex	3.77	4.13	8.31	0.36
Prelimbic cortex	5.07	0.09	3.21	2.52
Sensory cortex	3.89	−4.15	2.49	−0.36
Striatum	5.11	−4.01	2.96	−0.60

peak coordinates of the point of maximum effect in Paxinos and Watson space, in which the x-axis is negative to the left of the midline and positive to the right, the y-axis is positive ventrally and negative dorsally, and the z-axis is positive in the direction of the olfactory bulb relative to the bregma and negative in the direction of the cerebellum. Brain regions with significantly decreased glucose activity (reflecting increased glucose metabolism) were fused on structural slices of the rat brain using the Paxinos and Watson atlas (figure 2).

As shown in table 1, significantly decreased glucose metabolism was found on both the first and 30th day in the AD group compared with the control group in the following cerebral regions: hippocampus, dorsal thalamus, striatum, piriform cortex, and sensory cortex (figure 2A, B).

Higher rates of glucose metabolism in the hippocampus, orbital cortex, cerebellum, piriform cortex, retrosplenial cortex, sensory cortex, and olfactory cortex were found in the AD+HT7 group compared with the AD group after the 20th treatment (table 2, figure 2C, D).

The AD+HT7 group also demonstrated increased glucose metabolism compared with the AD+Sham group in the hippocampus, dorsal thalamus, olfactory cortex, cerebellum, pontine, and dentate gyrus (table 3, figure 2E, F).

Table 2 Brain regions demonstrating increased cerebral glucose metabolism of different regions in AD+HT7 versus AD groups

Anatomical structures	Max_T	Peak coordinates (mm) X	Y	Z
After 1st treatment				
Cerebellum—anterior lobe	4.21	2.69	4.92	−11.88
Cerebellum—posterior lobe	3.71	2.96	4.94	−11.88
Dorsal thalamus—lateral nucleus group	4.05	−2.37	6.96	−3.48
Hypothalamus—mammillary region	5.07	0.04	7.26	−3.72
Hypothalamus—tuberal region	3.84	−1.84	7.53	−3.00
Midbrain—substantia nigra	4.59	−2.75	7.48	−4.68
Midbrain—tegmentum of midbrain	3.75	2.20	7.24	−5.40
Orbital cortex	5.15	−1.81	3.25	4.20
Piriform cortex	3.65	2.76	7.04	2.28
Prelimbic cortex	3.92	−1.27	3.32	3.72
Striatum	4.13	−2.43	7.89	0.84
After 20th treatment				
Cerebellum—posterior lobe	4.11	3.48	2.86	−11.16
Hippocampus	3.83	−6.08	6.04	−5.40
Infralimbic cortex	4.29	−0.86	4.26	3.24
Olfactory cortex	4.48	−6.36	6.25	−4.68
Orbital cortex	4.06	−0.60	4.36	3.96
Prelimbic cortex	4.59	−0.99	3.84	3.00
Retrosplenial cortex	3.62	−1.40	1.51	−5.64
Visual cortex	4.10	−2.33	1.21	−6.12

AD, Alzheimer's disease.

Table 3 Brain regions demonstrating increased cerebral glucose metabolism of different regions in AD+HT7 versus AD+Sham groups

Anatomical structures	Max_T	Peak coordinates (mm) X	Y	Z
After 1st treatment				
Dorsal thalamus—lateral nucleus group	4.18	2.32	7.12	−3.96
After 20th treatment				
Amygdaloid body	3.51	−4.12	7.06	−2.52
Cerebellum—anterior lobe	4.30	0.53	6.42	−10.44
Cerebellum—posterior lobe	5.09	−3.59	4.87	−12.12
Dentate gyrus	5.35	−4.33	4.93	−6.60
Dorsal thalamus—lateral nucleus group	4.82	−3.67	4.90	−5.88
Hippocampus	5.99	−4.32	4.85	−7.32
Olfactory cortex	5.36	−4.44	4.90	−8.04
Pontine—tegmentum of pons	3.77	1.06	6.87	−10.20
Retrosplenial cortex	3.54	−3.10	2.29	−9.00
Striatum	4.01	−4.13	6.58	−2.04

AD, Alzheimer's disease.

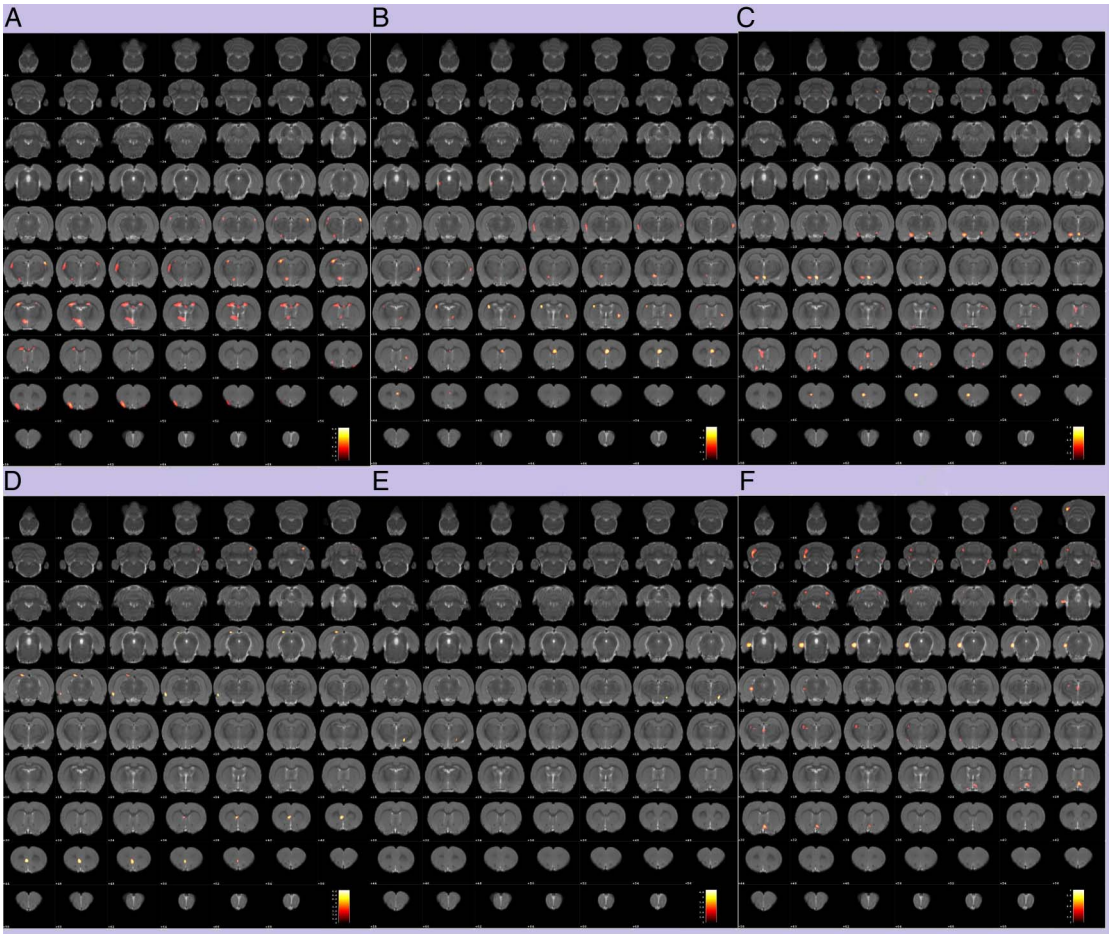

Figure 2 Graphical presentation of ^{18}F-2-fluoro-deoxy-D-glucose positron emission tomography (^{18}F-FDG-PET) scan results from 10 healthy rats (control group, n=10) and 36 rats with Alzheimer's disease (AD) left untreated (AD group, n=12) or treated with 20 sessions of acupuncture at HT7 (AD+HT7 group, n=12) or a distant non-acupuncture point (AD+Sham group, n=12) over a 30-day period. Results overlaid on a coronal view of rat brain and mapped to the Paxinos and Watson rat brain atlas. (A and B) Control versus AD groups. (C and D) AD+HT7 versus AD groups. (E and F) AD+HT7 versus AD+Sham groups. Colour bars represent the t value of each significant voxel.

DISCUSSION

In the present study, a Y-maze was used to test the memory skills of AD rats treated with acupuncture compared with healthy controls. AD weakened the ability of rats to remember the routes to the safe zone and to react instantly to electric shocks (reflected by increased TRT).

It is well known that the hippocampus plays an important role in the processing and recall of spatial and contextual information. This hippocampus-dependent spatial memory processing can be tested by the Y-maze behavioural task, which has been validated as a specific and sensitive test of spatial recognition memory in rodents.[16] The test relies on the innate tendency of rats to explore a novel environment. The Y-maze used in this study involved electric stimuli and was considered suitable for evaluating memory in the rats.[17] Previous neuroimaging studies have shown that the hippocampus is one of the earliest sites of neurodegeneration in AD and usually exhibits atrophy, hypometabolism, and decreased activity.[18] Herein, a low rate of ^{18}F-FDG uptake in the hippocampus was observed in AD rats compared with healthy controls; however this increased after acupuncture at HT7, which suggests that hypometabolism in the hippocampus, possibly associated with memory impairment, could be alleviated by needling HT7.

In the present study, it is noteworthy that the dorsal thalamus showed increased glucose metabolic activity during both the first and 20th treatments in AD +HT7 versus AD+Sham groups, which may represent an acute stress reaction. Several studies have demonstrated accumulation of abnormal iron deposits and increased microglial staining in the thalamus after acute injury. On the one hand, the potentially negative contribution of microglia to neurodegenerative disorders is supported by findings in AD, which suggest that stress plays an important role in microglial activation and can be inhibited by suppression of microglial activation. On the other hand, since iron is a catalyst for redox reactions, which can produce free radicals that induce tissue damage, its potential role in AD is

currently being explored. Iron participates in many enzymatic processes and exerts effects on the dopamine D2 receptor, which plays an important role in the expression of delta FosB and c-Fos.[19] Studies have also revealed that increased expression of c-Fos results in neuronal death via apoptosis. Interestingly, exposure to stress has been shown to lead to an increase in Fos-immunoreactive neurons in the hypothalamic paraventricular nucleus.[20] In the current study, altered glucose metabolism was found in the hypothalamus after the first treatment in AD+HT7 versus AD groups, indicating that the initial treatment effect of acupuncture influenced the dorsal thalamus and hypothalamus. Whether this is accompanied by microglial deactivation, decreased iron levels, and/or reduced c-Fos expression in these brain areas remains unknown.

Recently, with the help of voxel-based morphometry (VBM), the assessment of grey matter volume changes has been available for AD patients. Recent studies have reported diminished hippocampal and thalamic volumes in AD and AD-related regional atrophy in the anteromedial regions of the thalamus bilaterally and in the medial area of the left hippocampus.[21 22] It has been suggested that impairment of connections between the anterior thalamus and hippocampus (direct via the fornix and/or indirect via the mammillary bodies) is associated with AD-related memory loss.[23] Atrophy of these structures is not independent, rather primary neurodegeneration in one of the structures may lead to secondary degeneration of connected regions.[24] We hypothesise that acupuncture at HT7 prevents atrophy and degeneration of these regions by increasing regional glucose metabolism, which in turn slows progress of the disease and further improves memory and cognition ability.

To elucidate the effects of a course of acupuncture treatment, cerebral glucose metabolism was quantified at day 30 and compared with day 1 in AD+HT7 versus AD and AD+Sham groups. We found that the olfactory bulb, frontal lobe and temporal lobe may represent longer term target regions following needling at HT7. While atrophy of these regions has also been found in AD patients, it might be explained by the close connection among them.[25] Interestingly, a recent study suggested that cerebrospinal fluid (CSF) flows through olfactory CSF conduits (OCC), which run from the medial temporal lobe (MTL) along the lateral olfactory stria, through the olfactory trigon, and down the olfactory tract to the olfactory bulb. Olfactory dysfunction, involved in memory impairment, is common in AD. Reductions in OCC flow may impact CSF hydrodynamics upstream in the MTL and basal forebrain, resulting in less efficient Aβ removal from these areas and a deterioration of the neuropathological condition in AD.[26] Based on the relationship between memory formation and neuropathic changes in AD, we speculate that needling at HT7 impacts multiple regions including the hippocampus, thalamus, hypothalamus, frontal lobe, and temporal lobe.

However, the interpretation of aberrant metabolism in AD and the therapeutic mechanisms underlying acupuncture treatment remain uncertain. Depressed cerebral blood flow (CBF) regulation has been observed in AD patients,[27] and acupuncture treatment may increase CBF and improve hippocampal connectivity.[28] In rats, acupuncture stimulation also increases CBF.[29] Thus, reduced cerebral glucose metabolism might be associated with decreased CBF in AD and might be attenuated by acupuncture. The effects of acupuncture could also be explained by its ability to reverse decreased acetylcholine neurotransmission, improve synaptic transmission, and decrease oxidative damage in the hippocampus and related brain regions.[30] Oxidative damage has been linked with neurodegeneration and may reflect altered protein levels and antioxidant enzyme activity in the hippocampus.[31] Among markers of oxidative damage, iPF2α, a sensitive and specific marker of lipid peroxidation, is elevated in the hippocampus[32] and correlates with cognitive and functional impairment in patients with AD. Decreased levels of iPF2α have been demonstrated in CSF, blood, and urine of AD patients following acupuncture, suggesting an antioxidant effect of acupuncture within the brain.[33]

In this study, we deliberately chose a distant sham (non-acupuncture) point, as needling at a point anatomically close to HT7 may have stimulated the same nerve, spinal segment, and similar cortical regions. While HT7 is associated with the medial cutaneous nerve of the forearm, which is derived from the C8 and T1 spinal nerves, our chosen sham point is associated with the superficial fibular nerve, which is derived from the L4, L5, S1, and S2 roots. By needling at completely different points, we gained a better perspective of the regional effects of needling at HT7.

Our study has several limitations, however. Firstly, to induce our AD model, we chose intraperitoneal injection of D-gal combined with injection of IBO into the NBM based on our previous study.[34] This AD rat model mimics certain symptoms of AD (neurodegeneration[35] and memory impairment[36]) but lacks tangle formation and neuronal loss. Secondly, we were unable to directly explain the relationship between cerebral metabolic activity and prognosis in AD. The meaning of altered glucose metabolism in different brain regions following acupuncture needs to be clarified. In the future, we will examine these regions independently by choosing specific PET tracers and hopefully provide a better understanding of the therapeutic effects of acupuncture on AD.

In conclusion, we have shown that weakened memory abilities associated with AD can be improved by needling HT7 in a rat model of the condition. Cerebral glucose metabolic activity (measured using

^{18}F-FDG-PET technology) in the hippocampus, thalamus, hypothalamus, frontal lope, and temporal lobe were increased after acupuncture treatment in AD rats, and these effects have several possible explanations. Further investigations are required to further elucidate the mechanisms of action underlying acupuncture and altered glucose metabolic activity.

Acknowledgements This work was supported by the National 973 Programs of China grant number 2006CB504505 & 2012CB518504 and the National Nature Science Foundation of China grant number 90709027.

Contributors XL, YH and CT conceived and coordinated the study. YH and CT participated in the design of the study. JR finished the manuscript. YL, SC and JC performed the study. BS and BN performed the data analysis. All authors read and approved the final manuscript.

Funding The National 973 Programs of China (2012CB518504 and 2006 CB504505).

Competing interests None declared.

Provenance and peer review Not commissioned; externally peer reviewed.

REFERENCES

1 Yang C, Liu Y, Ni X, *et al*. Enhancement of the nonamyloidogenic pathway by exogenous NGF in an Alzheimer transgenic mouse model. *Neuropeptides* 2014;48:233–8.
2 Cummings JL, Isaacson RS, Schmitt FA, *et al*. A practical algorithm for managing Alzheimer's disease: what, when, and why? *Ann Clin Transl Neurol* 2015;2:307–23.
3 Sindi IA, Dodd PR. New insights into Alzheimer's disease pathogenesis: the involvement of neuroligins in synaptic malfunction. *Neurodegener Dis Manag* 2015;5:137–45.
4 Hughes TM, Craft S, Lopez OL. Review of the potential role of arterial stiffness in the pathogenesis of Alzheimer's disease. *Neurodegener Dis Manag* 2015;5:121–35.
5 Liang P, Wang Z, Qian T, *et al*. Acupuncture stimulation of Taichong (Liv3) and Hegu (LI4) modulates the default mode network activity in Alzheimer's disease. *Am J Alzheimers Dis Other Demen* 2014;29:739–48.
6 Lee MS, Shin BC, Ernst E. Acupuncture for Alzheimer's disease: a systematic review. *Int J Clin Pract* 2009;63:874–9.
7 Gu W, Jin XX, Zhang YJ, *et al*. Clinical observation of Alzheimer's disease treated with acupuncture. *Zhongguo Zhen Jiu* 2014;34:1156–60.
8 Wang Z, Nie B, Li D, *et al*. Effect of acupuncture in mild cognitive impairment and Alzheimer disease: a functional MRI study. *PLoS One* 2012;7:e42730.
9 Zhou Y, Jin J. Effect of acupuncture given at the HT 7, ST 36, ST 40 and KI 3 acupuncture points on various parts of the brains of Alzheimer's disease patients. *Acupunct Electrother Res* 2008;33:9–17.
10 Barthel H, Seibyl J, Sabri O. The role of positron emission tomography imaging in understanding Alzheimer's disease. *Expert Rev Neurother* 2015;15:395–406.
11 Catafau AM, Bullich S. Amyloid PET imaging: applications beyond Alzheimer's disease. *Clin Transl Imaging* 2015;3:39–55.
12 Kobylecki C, Langheinrich T, Hinz R, *et al*. 18F-florbetapir PET in patients with frontotemporal dementia and Alzheimer disease. *J Nucl Med* 2015;56:386–91.
13 Jang I, Cho K, Moon S, *et al*. A study on the central neural pathway of the heart, Nei-Kuan (EH-6) and Shen-Men (He-7) with neural tracer in rats. *Am J Chin Med* 2003;31:591–609.
14 Nie B, Liu H, Chen K, *et al*. A statistical parametric mapping toolbox used for voxel-wise analysis of FDG-PET images of rat brain. *PLoS One* 2014;9:e108295.
15 Paxinos G, Watson C. *The rat brain in stereotaxic coordinates*. 6 edn. New York: Academic Press, 2008.
16 Ghofrani S, Joghataei MT, Mohseni S, *et al*. Naringenin improves learning and memory in an Alzheimer's disease rat model: insights into the underlying mechanisms. *Eur J Pharmacol* 2015;764:195–201.
17 Hritcu L, Noumedem JA, Cioanca O, *et al*. Methanolic extract of Piper nigrum fruits improves memory impairment by decreasing brain oxidative stress in amyloid beta(1–42) rat model of Alzheimer's disease. *Cell Mol Neurobiol* 2014;34:437–49.
18 Mufson EJ, He B, Nadeem M. Hippocampal proNGF signaling pathways and [beta]-amyloid levels in mild cognitive impairment and Alzheimer disease. *J Neuropathol Exp Neurol* 2012;71:1018–29.
19 Nestler EJ. Transcriptional mechanisms of addiction: role of Delta FosB. *Philos Trans R Soc Lond B Biol Sci* 2008;363:3245–55.
20 Chowdhury GM, Fujioka T, Nakamura S. Induction and adaptation of Fos expression in the rat brain by two types of acute restraint stress. *Brain Res* 2000;52:171–82.
21 Štěpán-Buksakowska I, Szabó N, Hořínek D, *et al*. Cortical and subcortical atrophy in Alzheimer disease: parallel atrophy of thalamus and hippocampus. *Alzheimer Dis Assoc Disord* 2014;28:65–72.
22 Zarei M, Patenaude B, Damoiseaux J, *et al*. Combining shape and connectivity analysis: an MRI study of thalamic degeneration in Alzheimer's disease. *Neuroimage* 2010;49:1–8.
23 Colnat-Coulbois S, Mok K, Klein D, *et al*. Tractography of the amygdala and hippocampus: anatomical study and application to selective amygdalohippocampectomy. *J Neurosurg* 2010;113:1135–43.
24 Yuan TF, Slotnick BM. Roles of olfactory system dysfunction in depression. *Prog Neuropsychopharmacol Biol Psychiatry* 2014;54:26–30.
25 Ethell DW. Disruption of cerebrospinal fluid flow through the olfactory system may contribute to Alzheimer's disease pathogenesis. *J Alzheimers Dis* 2014;41:1021–30.
26 Thomann PA, Dos Santos V, Seidl U, *et al*. MRI-derived atrophy of the olfactory bulb and tract in mild cognitive impairment and Alzheimer's disease. *J Alzheimers Dis* 2009;17:213–21.
27 Di Marco LY, Venneri A, Farkas E, *et al*. Vascular dysfunction in the pathogenesis of Alzheimer's disease—a review of endothelium-mediated mechanisms and ensuing vicious circles. *Neurobiol Dis* 2015;82:593–606.
28 Wang Z, Liang P, Zhao Z, *et al*. Acupuncture modulates resting state hippocampal functional connectivity in Alzheimer disease. *PLoS One* 2014;9:e91160.
29 Uchida S, Kagitani F, Suzuki A, *et al*. Effect of acupuncture-like stimulation on cortical cerebral blood flow in anesthetized rats. *Jpn J Physiol* 2000;50:495–507.

30 Zhang P, Guan SS, Jiang GH. Effects of electroacupuncture on expression of Abeta positive cells of the hippocampus and SOD activity in rats with streptozocin-Alzheimer's disease. *Zhongguo Zhen Jiu* 2010;30:1007–10.
31 Bonda DJ, Wang X, Perry G, *et al*. Oxidative stress in Alzheimer disease: a possibility for prevention. *Neuropharmacology* 2010;59:290–4.
32 Sultana R, Piroddi M, Galli F, *et al*. Protein levels and activity of some antioxidant enzymes in hippocampus of subjects with amnestic mild cognitive impairment. *Neurochem Res* 2008;33:2540–6.
33 Pratico D, Clark CM, Lee VM, *et al*. Increased 8,12-iso-iPF2alpha-VI in Alzheimer's disease: correlation of a noninvasive index of lipid peroxidation with disease severity. *Ann Neurology* 2000;48:809–12.
34 Zhong ZG, Qu ZQ, Wang NP, *et al*. Effects of the Panax notoginseng saponins on the level of synaptophysin protein in brain in rat model with lesion of Meynert. *Zhongguo Zhong Yao Za Zhi* 2005;30:913–15.
35 Yamamoto M, Chikuma T, Kato T. Changes in the levels of neuropeptides and their metabolizing enzymes in the brain regions of nucleus basalis magnocellularis-lesioned rats. *J Pharmacol Sci* 2003;92:400–10.
36 Zhang XL, Jiang B, Li ZB, *et al*. Catalpol ameliorates cognition deficits and attenuates oxidative damage in the brain of senescent mice induced by D-galactose. *Pharmacol Biochem Behav* 2007;88:64–72.